Available online at www.sciencedirect.com
ScienceDirect
Trans. Nonferrous Met. Soc. China 22(2012) 1647−1654
Transactions of Nonferrous Metals Society of China
www.tnmsc.cn

Preparation and performance of coating on rare-earth compounds-immersed magnesium alloy by micro-arc oxidation

LIU Feng[1, 2], LI Yu-jie[1], GU Jia-jing[1], YAN Qing-song[2], LUO Qiang[1], CAI Qi-zhou[1]

1. State Key Laboratory of Material Processing and Die and Mould Technology, Huazhong University of Science and Technology, Wuhan 430074, China;
2. National Defense Key Disciplines Laboratory of Light Alloy Processing Science and Technology, Nanchang Hangkong University, Nanchang 330063, China

Received 21 July 2011; accepted 16 January 2012

Abstract: A composite ceramic coating containing Y_2O_3−ZrO_2−MgO (YSZ−MgO) was prepared on AZ91D magnesium alloy, which was immersed in $Y(NO_3)_3$ aqueous solution as pretreatment, by micro-arc oxidation (MAO) process. The morphology, elemental and phase compositions, corrosion behavior and thermal stability of the coatings were studied by SEM, EDX, XRD, electrochemical corrosion test, high temperature oxidation and thermal shock test. The results show that the coating mainly consists of ZrO_2, Y_2O_3, MgO, Mg_2SiO_4, and MgF_2. Among these compounds, Y_2O_3 accounts for 26.7% of (Y_2O_3 + ZrO_2). The thickness of YSZ−MgO coating is smaller than that of ZrO_2−MgO coating, but its compactness and surface roughness are better than those of ZrO_2−MgO coating. YSZ−MgO coating has a good corrosion resistance, and its corrosion rate in 5% NaCl aqueous solution is lower than that of ZrO_2−MgO and only about 8.5% of that of AZ91D magnesium alloy. After oxidation at 410 °C, the mass gain of AZ91D magnesium alloy presents a linear increase with the oxidation time. The YSZ−MgO coating and ZrO_2−MgO coating can remarkably decrease the oxidation mass gain. The oxidation mass gain of YSZ−MgO coating is lower than that of ZrO_2−MgO coating, especially during a long oxidation period. The thermal shock resistance of YSZ−MgO coating is superior to ZrO_2−MgO coating.
Key words: AZ91D magnesium alloy; micro-arc oxidation (MAO); Y_2O_3−ZrO_2−MgO composite coating; corrosion behavior; thermal stability

1 Introduction

Magnesium alloys are promisingly applied in a number of domains including automotive, aerospace and computer and communication industries owing to their prominent characteristics, such as low density, high specific strength and stiffness. However, the applications of magnesium alloy are seriously restricted by their poor corrosion resistance and heat resistance. It is necessary for magnesium alloy products to adopt proper surface protective treatment [1−4].

Micro-arc oxidation (MAO) has been generally recognized as one of the most prospective methods of surface treatment for magnesium alloys. Ceramic coatings can be in situ formed on magnesium alloys after the MAO process in the common silicate electrolyte and the coatings are mainly composed of MgO, Mg_2SiO_4 and $MgAl_2O_4$. The coatings exhibit high hardness, high wear resistance and excellent electromagnetic shielding characteristics, etc [5]. Unfortunately, they will easily crack and fall off, which makes magnesium alloy lose protection since these composite oxide ceramic coatings show high brightness and their coefficients of linear expansion are remarkable different from that of magnesium alloy.

Y_2O_3−ZrO_2−MgO (YSZ−MgO) composite ceramic coatings are prospective to applying in protecting metal substrates for excellent corrosion resistance, thermal stability, low thermal conductivity and high coefficient of thermal expansion, and more, they show specific micro-crack toughening and phase transformation toughening mechanism [6,7]. However, it is difficult to achieve an optimal Y_2O_3 content in Y_2O_3−ZrO_2−MgO composite ceramic coatings by common MAO process [8]. In this work, the YSZ−MgO coating was prepared on an AZ91D magnesium alloy through MAO process by first immersing the magnesium alloy in $Y(NO_3)_3$ aqueous

Foundation item: Project (gf200901002) support by the National Defense Key Disciplines Laboratory of Light Alloy Processing Science and Technology of Nanchang Hangkong University, China
Corresponding author: CAI Qi-zhou; Tel: +86-27-87558190; E-mail: caiqizhou@mail.hust.edu.cn; YAN Qing-song; Tel: +86-791-3953326; E-mail: yanqs1973@126.com
DOI: 10.1016/S1003-6326(11)61368-X

solution. The microstructure, phase composition, corrosion resistance and thermal stability of the composite ceramic coating were investigated.

2 Experimental

Specimens with dimensions of 10 mm×10 mm×10 mm and 50 mm×25 mm×7 mm were cut from metal cast AZ91D magnesium alloy (9.21%Al, 0.63%Zn, 0.29%Mn, Mg balance, in mass fraction). The specimen of 10 mm×10 mm×10 mm was used for polarization curve and thermal shock test, and the specimens of 50 mm×25 mm×7 mm was used for full-soak corrosion and high-temperature oxidation test. All specimens were polished to a grit of 2000 by SiC papers, and then degreased in acetone and distilled water.

The pretreatment of magnesium alloy was carried out by immersing the specimens into 7.5 g/L $Y(NO_3)_3$ aqueous solution for a period of 5 min, then dried in air.

An aqueous solution containing K_2ZrF_6−Na_2SiO_3 was used as the electrolyte and used for MAO process. The experimental parameters were as follows: anodic voltage 330 V, cathodic voltage −60 V, frequency 700 Hz, duty ratio 30%, electrolyte temperature 25−40 °C, oxidation time 10 min and the pH value of electrolyte 13.05. Y_2O_3−ZrO_2−MgO ceramic coating (YSZ−MgO) with immersing pretreatment and ZrO_2−MgO ceramic coating without immersing pretreatment were prepared by this system. The ZrO_2−MgO ceramic coating was used for the comparison test.

Table 1 Composition and concentration of electrolyte

Composition	Concentration/(g·L^{-1})
Na_2SiO_3	10−20
K_2ZrF_6	10−25
$C_3H_8O_3$	4−6
KOH	5−15
KF	3−10

Surface and cross-sectional morphologies of the coating were examined by environmental scanning electron microscope (Quanta 200, FEI Co. Eindhoven, the Netherlands). The elemental composition of the samples was analyzed by energy dispersive X-ray spectrometer (EDX: INCA 350 Energy, Oxford Instrument GmbH, Wiesbaden, Germany). The phase composition of the samples was detected by X-ray diffractometer (XRD: X pert PRO, PANalytical, the Netherlands) with Cu K_α radiation (λ=1.54060 Å) and the detected angle (2θ) was scanned from 10° to 90° with 0.02° steps.

The corrosion resistance of YSZ−MgO and ZrO_2−MgO coatings was evaluated by potentiodynamic polarization test in 3.5% NaCl aqueous solution and the full-soak corrosion test in 5% NaCl solution. The potentiodynamic polarization test was performed on IM6ex electrochemical workstation. The scanning range was from −200 mV to 200 mV with a scanning rate of 2 mV/s. The time for the full-soak corrosion test was 120 h, and the mass loss method was used for evaluating the corrosion rate of the coatings.

The high temperature oxidation test of the coatings was conducted at 410 °C in a muffle furnace (type SX2−8−13), and then cooled off in the air. High temperature oxidation resistance of the samples was evaluated by mass gain method. In the thermal shock test, samples were preserved at 500 °C for 5 min in the muffle furnace, and then quickly immersed into distilled water at room temperature. This process was repeated several times. The thermal shock resistance was evaluated by the repetition times when the first crack appeared and the coating began to fall off.

3 Results and discussion

3.1 Surface morphology of pretreated specimen

The surface morphology and EDX spectrum of pretreated specimen are shown in Fig. 1. The composition of costing is listed in Table 2. From Fig. 1 and Table 2, it can be seen that the coating formed during

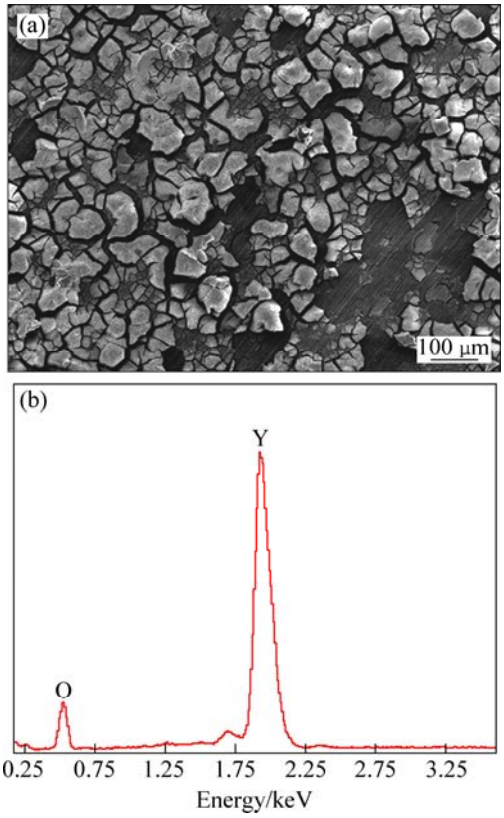

Fig. 1 SEM image showing surface morphology (a) and EDX spectrum (b) of pretreated coating

pretreatment process is full of cracks and consists of Y and O elements. The XRD pattern of the coating is shown in Fig. 2. It can be found that the coating contains Y_2O_3 after immersion. When the magnesium alloy is immersed in $Y(NO_3)_3$ aqueous solution, the reaction between magnesium and $Y(NO_3)_3$ solution is similar with the hydrogen evolution reaction between inactive metals and strong alkali solutions because the electronegativity of magnesium is more negative than that of yttrium. The chemical reactions below occurred in the immersion process:

$$3H_2O + Y(NO_3)_3 \rightarrow 3HNO_3 + Y(OH)_3 \downarrow \quad (1)$$

$$Mg + 2HNO_3 \rightarrow Mg(NO_3)_2 + H_2 \uparrow \quad (2)$$

$$2Y(OH)_3 \rightarrow Y_2O_3 + 3H_2O \quad (3)$$

Table 2 Elemental composition of pretreated coating (EDX)

Element	*w*/%	*x*/%
Y	74.03	33.91
O	25.97	66.09

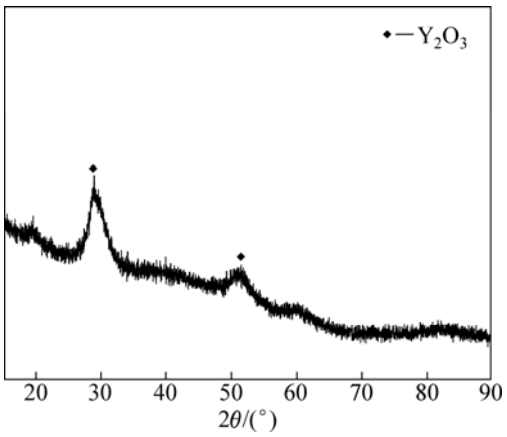

Fig. 2 XRD pattern of pretreated coating

Before immersion, reaction (1) takes place in $Y(NO_3)_3$ aqueous solution, but the reaction rate is rather low. When the specimen is soaked in the solution, reaction (2) occurs, the surface of magnesium alloy is covered by small bubbles. Consequently, reaction (1) is promoted by reaction (2). And $Y(OH)_3$ partly converts Y_2O_3 by dehydration reaction (shown in reaction (3)).

3.2 Surface and cross-sectional morphologies of MAO coatings

The surface morphologies of YSZ−MgO coating and ZrO_2−MgO coating are shown in Fig. 3. It shows that there are residual discharging micro-pores on the surface of the coating after the MAO process. These micro-pores are not only the reaction channels between the solution and the substrate, but also the channels from which melting oxides erupt out during the reaction

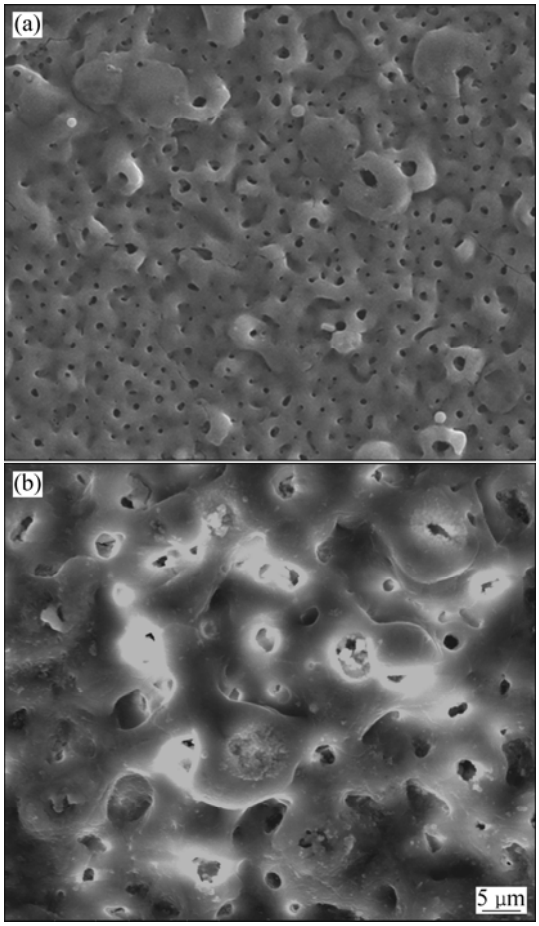

Fig. 3 SEM images showing surface morphologies of MAO coatings: (a) YSZ−MgO coating ; (b) ZrO_2−MgO coating

period. From Fig. 3, it can be seen that the micro-pores of ZrO_2−MgO coating are larger in size and fewer in number than YSZ−MgO coating, while the micro-pores of YSZ−MgO coating are well distributed. This phenomenon may be due to the relatively stable plasma-arc and a decrease in melting point of oxides. The fused oxides are prone to flow and the gases become facile to escape.

Cross-sectional morphologies of YSZ−MgO coating and ZrO_2−MgO coating are shown in Fig. 4. It shows that the thickness of YSZ−MgO coating is smaller than that of ZrO_2−MgO coating, and YSZ−MgO coating has better compactness. This is because the electric breakdown on the surface is hindered when the surface of the sample is covered by ceramic coating containing rare earth elements in the MAO process. At the initial stage of MAO process, the ceramic coating is mainly composed of MgO. MgO shows high melting point and viscosity while both of them decrease for the permeating of rare earth oxides. It is beneficial to seal discharge channels and to escape gas in fused oxides. Meanwhile, rare earth oxides restrain the growth of ceramic crystals and refine the grain [9,10].

3.3 Phase and elemental compositions

The surface morphology and EDX spectrum of YSZ−MgO coating are shown in Fig. 5 and the elemental compositions are listed in Table 3. As shown in Fig.5 and Table 3, the coating consists of O, F, Na, Mg, Al, Y, Zr and K elements. The elements of Na and K come from Na^+ and K^+ in electrolyte. Moreover, ZrF_6^{2-} in the electrolyte participated in reaction of the coating formation. From Table 3, it can be calculated that Y_2O_3 accounts for 26.78% of Y_2O_3+ZrO_2 in the coating according to the contents of Zr and Y elements.

The binary phrase diagram of ZrO_2−Y_2O_3 is shown in Fig. 6 [11]. It can be found from Fig. 6, the phase transition temperature decreases and forms a temperature interval when the stabilizer Y_2O_3 is added into ZrO_2 to constitute a binary system. It is necessary to add nearly 20% Y_2O_3 in order to transform ZrO_2 into steady cubic crystalline structure totally.

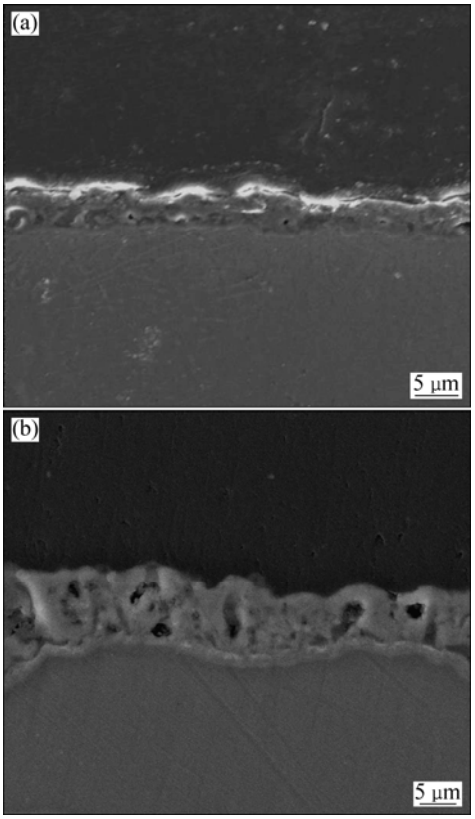

Fig. 4 SEM images showing cross-sectional morphologies of MAO coatings: (a) YSZ−MgO coating; (b) ZrO_2−MgO coating

Table 3 Elemental composition of YSZ−MgO coating

Element	*w*/%	*x*/%
O	7.8	11.75
F	27.42	34.77
Na	1.18	1.23
Mg	41.88	41.50
Al	4.31	3.85
Y	3.22	0.87
Zr	8.24	2.18
K	5.25	3.24

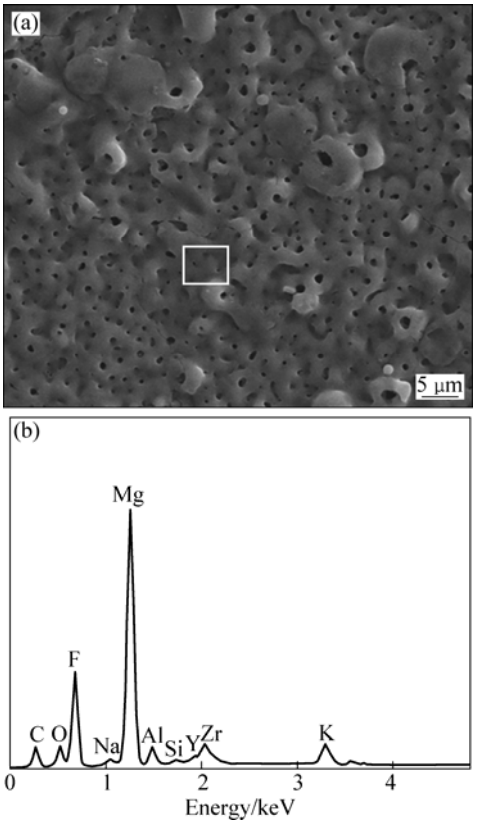

Fig. 5 SEM image showing surface morphology (a) and EDX spectrum (b) of YSZ−MgO coating

Previous experiments showed that the content of Y_2O_3 has little influence on thermal conductivity of ZrO_2, while greatly influencing the coefficient of thermal expansion of ZrO_2. ZrO_2 has three kinds of isomers under natural condition: from room temperature to about 1000 °C, ZrO_2 is in the monoclinic crystal structure (*m*-phrase); ZrO_2 will gradually transform into the tetragonal crystal structure (*t*-phase) when the temperature is over 1000 °C; ZrO_2 will totally turn into the cubic crystal structure (*c*-phase) when the temperature is above 1170 °C. As shown in Fig. 6, the crystal structure of ZrO_2 changes ($t \rightarrow m$) during the process of thermal cycling when the Y_2O_3 content is lower than 6%. As the temperature increases, $m \rightarrow t$ and it is accompanied with volume contraction for about 7%; whereas accompanied with volume expansion for more than 7%. The two processes mentioned above are both irreversible. Therefore, the change of volume after each cycling is also irreversible and keeps accumulating. As a result, the coating begins to crack and shed for the strong thermal stress. When the content of Y_2O_3 is between 6% and 8% (eutectic point), the stabilizing effect of Y_2O_3 is

the best owing to the counteraction of the volume contraction of $m \rightarrow t$ and the volume expansion of $t \rightarrow c$. ZrO_2 will only be *c*-phase and phase transition will cease ignoring the changes of temperature when the content of Y_2O_3 is over 20% [12−14].

The XRD analysis of MAO coatings is shown in Fig. 7. It displays that the normal ZrO_2−MgO coating is mainly composed of MgO, ZrO_2, MgF_2, Mg_2SiO_4, etc. YSZ−MgO coating is composed of MgO, ZrO_2, Y_2O_3, MgF_2, Mg_2SiO_4, etc. Y_2O_3 contained in YSZ−MgO coating can stabilize ZrO_2, and prevent the coating from cracking. On the other hand, ZrO_2 can toughen the MgO coatings and improve the heat shock resistance [15,16].

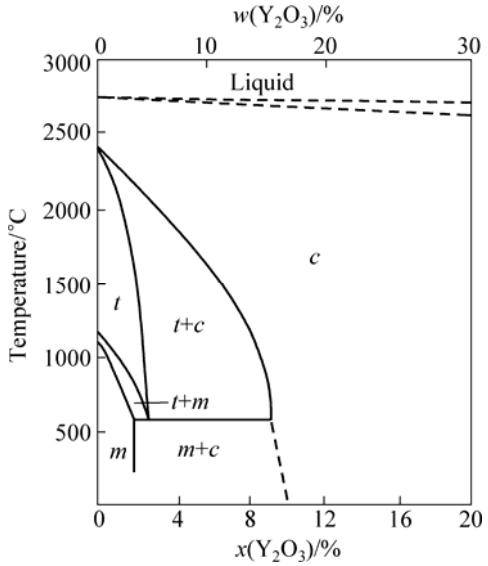

Fig. 6 Binary phase diagram of ZrO_2−Y_2O_3 [11]

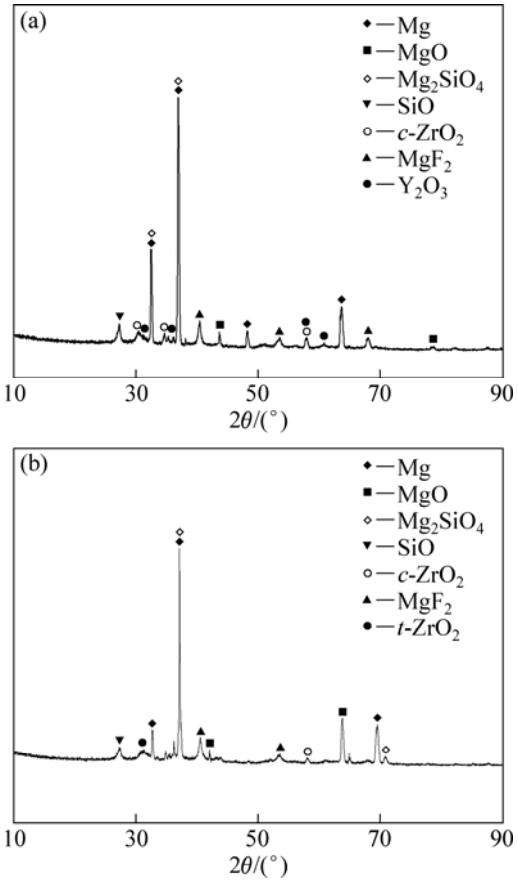

Fig. 7 XRD patterns of MAO coatings: (a) YSZ−MgO coating; (b) ZrO_2−MgO coating

When K_2ZrF_6 is added to the alkaline electrolyte for preparing YSZ−MgO coatings, reaction (4) occurs.

$$K_2ZrF_6 + 4KOH \rightarrow Zr(OH)_4 \downarrow + 6KF \quad (4)$$

The isoelectric point of $Zr(OH)_4$ colloidal particles is pH=6.8. When pH is less than 6.8, the colloidal particles are positively charged; when pH is larger than 6.8, the colloidal particles are negatively charged [17]. Therefore, $Zr(OH)_4$ particles negatively-charged in alkaline will move to the anode (AZ91D) in electric field and attach to the surface of specimens when the solution system is charged. Then, the high temperature and high pressure environment in discharge channel enhances reaction (5) and ZrO_2 is produced when plasma discharge occurs.

$$Zr(OH)_4 \rightarrow ZrO_2 + 2H_2O \quad (5)$$

3.4 Corrosion resistance

3.4.1 Potentiodynamic polarization test

The potentiodynamic polarization curves of AZ91D magnesium alloy, YSZ−MgO coating and ZrO_2−MgO coating in 3.5% NaCl solution are shown in Fig. 8. After the MAO process, the polarization curves of coated magnesium alloy shift to the left and its corrosion current density largely decreases under the same potential, as shown in Fig. 8. The polarization curves of AZ91D magnesium alloy before and after the MAO process are similar. However, in anode polarization interval, the corrosion current density of MAO coatings is lower than that of uncoated sample. This indicates that coatings restrain the corrosion process of magnesium alloy in

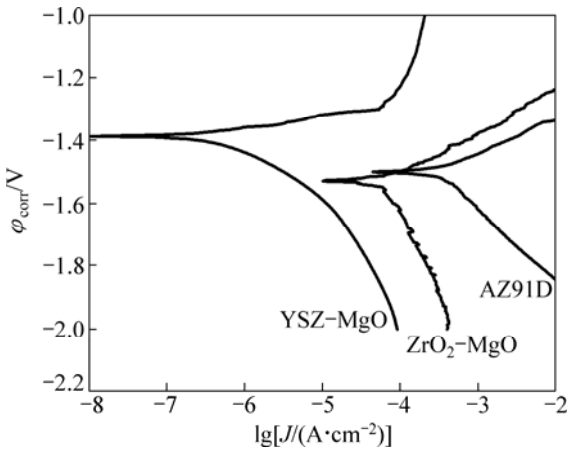

Fig. 8 Potentiodynamic polarization curves of magnesium and MAO coatings in 3.5% NaCl aqueous solution

anode and improve the corrosion resistance of magnesium alloy in chlorides. By comparing the curves of YSZ−MgO coating with ZrO_2−MgO coating, it can be found that YSZ−MgO coating shows lower corrosion current density and higher corrosion resistance.

The corrosion potential (φ_{corr}), corrosion current density (J_{corr}) and anode/cathode slope (b_a, b_c) were derived by Tafel fitting [18] from the polarization curves. Based on the data in Table 4, the polarization resistance R_p can be calculated by Stern−Gearyequation (Eq. (6)) [19]. The results are listed in Table 4.

$$R_p = \frac{b_a b_c}{2.303(b_a + b_c)} \cdot \frac{1}{J_{corr}} \quad (6)$$

Table 4 Tafel fitting results of potentiodynamic polarization curves

Sample	b_a/ (mV·dec^{-1})	b_c/ (mV·dec^{-1})	φ_{corr}/ V	J_{corr}/ (μA·cm^{-2})	R_p/ (kΩ·dec^{-1})
AZ91D	57.7	41.4	−1.503	145	0.722×10^2
ZrO_2−MgO	623	135	−1.531	54.9	8.774×10^3
YSZ−MgO	31.0	74.7	−1.384	0.187	5.087×10^4

The results in Table 4 suggest that the polarization resistance of MAO coatings is 2−3 magnitudes higher than that of uncoated magnesium alloy. This phenomenon further demonstrates that the corrosion resistance of magnesium alloy is remarkably improved after the MAO process. By comparing the fitting data of the two kinds of coatings, it is found that YSZ−MgO coating shows smaller corrosion current density, nobler open-circuit-potential (self-corrosion-potential) and higher polarization resistance. This demonstrates that YSZ−MgO coating has better corrosion resistance than ZrO_2−MgO coating.

3.4.2 Full soak corrosion in 5% NaCl aqueous solution

The corrosion rates of magnesium alloy and the two kinds of coatings in 5% NaCl solution for 120 h are shown in Table 5. As shown in Table 5, the corrosion rate of YSZ−MgO coating is lower than that of ZrO_2−MgO coatings and it is only 8.5% of AZ91D sample. This is because that the compactness of YSZ−MgO coating is much better than that of ZrO_2−MgO coating. Therefore, the YSZ−MgO coating can effectively prevent magnesium alloy from being corroded by corrosion medium.

Table 5 Corrosion rate of magnesium alloy and MAO coatings in 5% NaCl aqueous solution

Sample	Mass/g		Corrosion rate/ (g·m^{-2}·h^{-1})
	Before corrosion	After corrosion	
YSZ−MgO	17.8336	17.6039	0.461
ZrO_2−MgO	17.7489	17.0713	1.360
AZ91D	17.6129	14.8545	5.444

The micro-morphology of YSZ−MgO coating corroded in 5% NaCl aqueous solution for 120 h is shown in Fig. 9. From Fig.9, it can be seen that the corrosion pit appears on the YSZ−MgO coating, but obvious destruction is not detected on the surface.

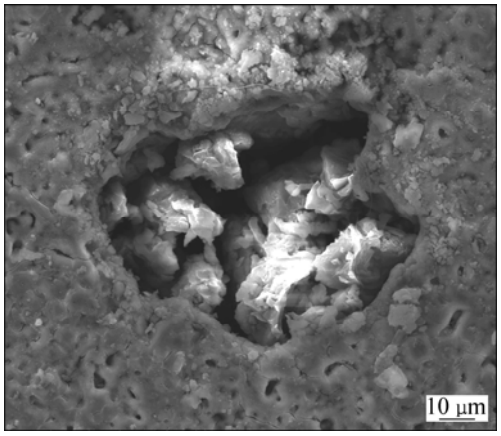

Fig. 9 SEM image showing surface morphology of YSZ−MgO coatings after immersion in 5% NaCl aqueous solution for 120 h

3.5 High temperature oxidation and thermal shock resistance

The mass gain curves of AZ91D magnesium alloy and the two kinds of coatings at 410 °C for different oxidation time are shown in Fig. 10. The mass gain of AZ91D magnesium alloy shows a quick increase with the time, but the mass gain remarkably decreases by MAO process. Compared ZrO_2−MgO coating with YSZ−MgO coating, the mass gain of YSZ−MgO coating is lower than that of ZrO_2−MgO coating, especially in a longer oxidation time.

The thermal shock resistances of ZrO_2−MgO and

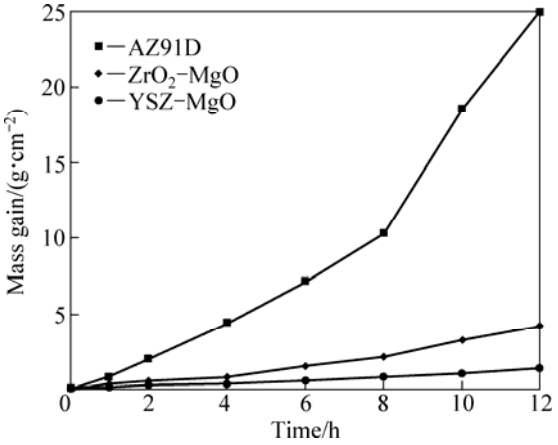

Fig. 10 Mass gain—time curves of samples after oxidation at 410 °C before and after MAO process

YSZ−MgO coatings are shown in Table 6. As shown in Table 6, the thermal shock resistance of YSZ−MgO coating is superior to ZrO_2−MgO coating.

Table 6 Result of thermal shock test of MAO coatings

Sample	N_1	N_2	N_3
ZrO_2−MgO	18	30	40
YSZ−MgO	23	45	55

N_1: Cycle number for the first cracking appearance; N_2: Cycle number for a few fall-off in the corners of the coating; N_3: Cycle number for large areas fall-off

It can be found from Fig. 10 and Table 6, YSZ−MgO coating is provided with a higher thermal shock resistance and fall-off resistance because the Y_2O_3 stabilized ZrO_2 can restrain the cracking tendency and improve the toughness of the coatings. Additionally, YSZ−MgO coating with a certain thickness of inner compact layer shows a higher bonding strength with substrate. Thus, the YSZ−MgO coating is not easy to crack or peel in thermal shock process. A small part of the coating falls off from the corner of the sample after a certain time of thermal cycling. This is because the growing process of coating after the MAO process is often accompanied by "edge effects", namely, vigorous point discharge occurs on the corner of the specimen, which makes the coating on the corner several or even over 10 times thicker than the coating in the middle. In addition, the radiated heat exchange is greater and the heat transfer channel of gas molecules is also shorter in the corners. As a result, more heat loss and faster cooling rate are available. Therefore, during the thermal shock process, fall-off occurs at the corner of the specimen [20,21]. When the coatings started to peel, they are hardly protective to substrate and lead to large areas fall-off.

4 Conclusions

1) A YSZ−MgO-containing composite ceramic coating was successfully prepared on AZ91D magnesium alloy by immersing in $Y(NO_3)_3$ aqueous solution as pretreatment before MAO process. The coating mainly consists of ZrO_2, Y_2O_3, MgO, Mg_2SiO_4 and MgF_2. Among these compounds, Y_2O_3 accounts for 26.7% of (Y_2O_3 + ZrO_2).

2) The thickness of YSZ−MgO coating is smaller than that of ZrO_2−MgO coating, but its compactness and surface roughness are better than those of ZrO_2−MgO coating.

3) YSZ−MgO coating shows a lower corrosion current density, nobler open circuit potentials and higher polarization resistance compared with the ZrO_2−MgO coating. When YSZ−MgO coating is soaked in 5% NaCl aqueous solution for 120 h, its corrosion rate is lower than that of ZrO_2−MgO and only about 8.5% of that of AZ91D magnesium alloy.

4) After oxidation at 410 °C, the mass gain of AZ91D magnesium alloy presents a linear increase with the oxidation time. The YSZ−MgO and ZrO_2−MgO coating can remarkably decrease the oxidation mass gain. The oxidation mass gain of YSZ−MgO coating is lower than that of ZrO_2−MgO coating, especially in a longer oxidation time. The thermal shock resistance of YSZ−MgO coating is superior to ZrO_2−MgO coating.

Acknowledgements

The authors gratefully thank Analytic and Testing Center of Huazhong University of Science and Technology for assistance in the specimen examination.

References

[1] YU Gang, LIU Yue-long, LI Ying. Corrosion and protection of magnesium alloys [J]. The Chinese Journal of Nonferrous Metals, 2002, 12(6): 1087−1097. (in Chinese)

[2] YANG Li-hui, LI Jun-qing, JIANG Wei-wei, ZHANG Mi-lin. Current status of surface treatment for magnesium and its alloys [J]. Journal of Chinese Society for Corrosion and Protection, 2008, 28(5): 316−319. (in Chinese)

[3] GAIA B, UGO B, ROBERTO B. About some corrosion mechanisms of AZ91D magnesium alloy[J]. Corrosion Science, 2005, 47: 2173−2184.

[4] YU Bing-lung, LIN Jun-kai, UAN Jun-yen. Applications of carbonic acid solution for developing conversion coatings on Mg alloy [J]. Transactions of Nonferrous Metals Society of China, 2010, 20: 1331−1339.

[5] JIANG Bai-ling, ZHANG Shu-jian, WU Guo-jian, LEI Ting-quan. Micro-defect and phase composition and corrosion of magnesium alloy by micro-arc oxidation [J]. The Chinese Journal of Nonferrous Metals, 2002, 12(6): 454−457. (in Chinese)

[6] CAI Qi-zhou, WANG Li-shi, WEI Bo-kang. Electrochemical performance of micro-arc oxidation films formed on AZ91D magnesium alloy in silicate and phosphate electrolytes [J]. Surface and Coatings Technology, 2006, 200: 3727−3733. (in Chinese)

[7] TIAN Yong-sheng, CHEN Chuan-zhong, LIU Jun-hong, LEI Ting-quan. The development of ZrO_2 thermal barrier coatings [J]. Chinese Mechanical Engineering, 2005, 16: 1449−1503.

[8] SHIRATORI Y, TIETZ F, BUCHKREMER H P, STOVER D. YSZ–MgO composite electrolyte with adjusted thermal expansion coefficient to other SOFC components [J]. Solid State Ionics, 2003, 164: 27−33.

[9] LUO Hai-he, CAI Qi-zhou, HE Jian, WEI Bo-kang. Preparation and properties of composite ceramic coating containing Al_2O_3−ZrO_2−Y_2O_3 on AZ91D magnesium alloy by plasma electrolytic oxidation [J]. Current Applied Physics, 2009, 9(6): 1341−1346.

[10] ZHU Hong, MU Bai-chun. Application of rare-earth element in ceramic materials [J]. Foshan Ceramics, 2007, 17(1): 35−39. (in Chinese)

[11] WANG Rui-gang, PAN Wei, CHEN Jian, JIANG Meng-ning, LUO Yong-ming, FANG Ming-hao. Properties and microstructure of machinable Al_2O_3/$LaPO_4$ ceramic composites [J]. Ceramics International, 2003, 29(1): 19−25. (in Chinese)

[12] DENG Shi-jun. Technology of high-performance ceramic coatings [M]. Beijing: Chemical Industry Press, 2004: 609−611. (in Chinese)

[13] FUNKE C, MAILAND J C, SIEBERT B. Characterization of ZrO_2−7wt%Y_2O_3 thermal barrier coatings with different parasites and FEM analysis of stress redistribution during thermal cycling of TBC [J]. Surface and Coatings Technology, 1997, 94−95: 106−112.

[14] SCHWINGEL D, TAYLOR R, HAUBOLD T, WIGREN J, GUALCO C. Mechanical and thermophysical properties of thick PYSZ thermal barrier coatings: correlation with microstructure and spraying parameters [J]. Surface and Coatings Technology, 1998, 108−109: 99−106.

[15] KHAN A N, LU J. Thermal cyclic behavior of air plasma sprayed thermal coatings sprayed on stainless steel substrates [J]. Surface and Coatings Technology, 2007, 201: 4653−4658.

[16] CHANG Li-min. Growth regularity of ceramic coating on magnesium alloy by plasma electrolytic oxidation [J]. Journal of Alloys and Compounds, 2009, 468: 462−465.

[17] JI Z, HAYNES J A, FERBER M K, RIGSBEE J M. Metastable tetragonal zirconia formation and transformation in reactively sputter deposited zirconia coatings [J]. Surface and Coatings Technology, 2001, 135: 109−117.

[18] XU Yu-fen, FAN Wen-yuan. Study on ceramic membrane separation of $Zr(OH)_4$ suspension [J]. China Powder Science and Technology, 2000, 6(Z1): 251−253. (in Chinese)

[19] CAO Chu-nan. Corrosion electrochemical theory [M]. Beijing: Chemical Industry Press, 1985. (in Chinese)

[20] YOU Guo-yan. Fundamental study on a novel technique of Mg shielding gas [D]. Chongqing: Chongqing University, 2007. (in Chinese)

[21] LI Mei-shuan. High temperature corrosion of metals [M]. Beijing: Metallurgical Industry Press, 2001. (in Chinese)

稀土盐浸泡镁合金微弧氧化膜层的制备及性能

刘 峰[1,2]，李玉洁[1]，顾佳婧[1]，严青松[2]，罗 强[1]，蔡启舟[1]

1. 华中科技大学 材料成形与模具技术国家重点实验室，武汉 430074；
2. 南昌航空大学 轻合金加工科学与技术国防重点学科实验室，南昌 330063

摘 要：在 K_2ZrF_6−Na_2SiO_3 电解液中对 $Y(NO_3)_3$ 浸泡预处理的 AZ91D 镁合金进行微弧氧化处理，在镁合金表面制备 Y_2O_3−ZrO_2−MgO 复合膜层(YSZ−MgO 膜)。运用电子显微镜(SEM)、能谱分析(EDX)、X 射线衍射(XRD)和电化学分析与高温氧化等方法研究 YSZ−MgO 膜的组成与结构、耐腐蚀性及热稳定性。结果表明，YSZ−MgO 膜主要由 Y_2O_3、ZrO_2、MgO 和 Mg_2SiO_4 等物相组成，和未经 $Y(NO_3)_3$ 浸泡的膜层(ZrO_2−MgO 膜)相比，YSZ−MgO 膜的厚度较小，但膜层的致密性较好，表面粗糙度较小；且腐蚀电流密度较小、开路电位较正、极化阻抗较高；在 5%NaCl 溶液中的腐蚀速率低于 ZrO_2−MgO 膜的，约为 AZ91D 镁合金的 8%。YSZ−MgO 膜层比普通 ZrO_2−MgO 膜层具有更强的抗高温氧化性能和耐热冲击性能。

关键词：AZ91D 镁合金；微弧氧化；Y_2O_3−ZrO_2−MgO 复合膜；腐蚀性能；耐热性

(Edited by LI Xiang-qun)